Formation characteristics and photoluminescence of Ge nanocrystals in HfO 2

Sung Kim, Sung Won Hwang, Suk-Ho Choi, R. G. Elliman, Young-Min Kim, and Youn-Joong Kim

Citation: Journal of Applied Physics **105**, 106112 (2009); doi: 10.1063/1.3132797
View online: http://dx.doi.org/10.1063/1.3132797
View Table of Contents: http://scitation.aip.org/content/aip/journal/jap/105/10?ver=pdfcov
Published by the AIP Publishing

Formation characteristics and photoluminescence of Ge nanocrystals in HfO_2

Sung Kim,[2] Sung Won Hwang,[1] Suk-Ho Choi,[1,a)] R. G. Elliman,[2] Young-Min Kim,[3] and Youn-Joong Kim[3]
[1]*Department of Applied Physics, College of Applied Sciences, Kyung Hee University, Yongin 449-701, Republic of Korea*
[2]*Department of Electronic Materials Engineering, Research School of Physical Sciences and Engineering, Australian National University, Canberra ACT 0200, Australia*
[3]*Division of Electron Microscopic Research, Korea Basic Science Institute, Daejeon 305-333, Republic of Korea*

(Received 31 January 2009; accepted 18 April 2009; published online 28 May 2009)

Ge nanocrystals (NCs) are shown to form within HfO_2 at relatively low annealing temperatures (600–700 °C) and to exhibit characteristic photoluminescence (PL) emission consistent with quantum confinement effects. After annealing at 600 °C, sample implanted with 8.4×10^{15} Ge cm^{-2} show two major PL peaks, at 0.94 and 0.88 eV, which are attributed to no-phonon and transverse-optical phonon replica of Ge NCs, respectively. The intensity reaches a maximum for annealing temperatures around 700 °C and decreases at higher temperatures as the NC size continues to increase. The no-phonon emission also undergoes a significant redshift for temperatures above 800 °C. For fluences in the range from 8.4×10^{15} to 2.5×10^{16} cm^{-2}, the average NC size increases from $\sim13.5\pm2.6$ to $\sim20.0\pm3.7$ nm. These NC sizes are much larger than within amorphous SiO_2. Implanted Ge is shown to form Ge NCs within the matrix of monoclinic (*m*)-HfO_2 during thermal annealing with the orientation relationship of [101]*m*-HfO_2 // [110]Ge NC. © *2009 American Institute of Physics*. [DOI: 10.1063/1.3132797]

Nanocrystal (NC) floating gate memories (NFGM) have received considerable attention as one of the most promising candidates for future nonvolatile, high-density, and low-power flash memory devices.[1,2] Both semiconducting and metallic NCs have been considered for charge storage.[1–3] Of the semiconductor candidates, Ge is of particular interest because NCs can be formed at relatively low temperatures (800–900 °C) and have a small bandgap.[4] The continued scaling of complementary metal-oxide-silicon (CMOS) technology has also recently seen a shift to high-dielectric-constant (high-*k*) dielectrics as a replacement for SiO_2 as the gate dielectrics.[5] Hf-based oxides are one of the most attractive high-*k* dielectrics due to their high permittivity and compatibility with CMOS processing.[6] This has led to an interest in the formation of NCs within HfO_2, including Ge NCs, for advanced CMOS technology.[7] The size and density of Ge NCs or SiGe nanodots (NDs) are known to be distributed nonuniformly within amorphous SiO_2 matrix due to the high diffusivity of Ge atoms.[8,9] In contrast, nucleation or aggregation of Ge atoms within Hf-based high-*k* matrix would be strongly influenced by the crystallization of the high-*k* matrix during thermal annealing because the Hf-based oxides are crystallized at lower temperatures than Ge. There have been almost no systematic studies on the growth and optical properties of Ge NCs within high-*k* dielectrics despite intense research on their NFGM application. In this communication, we report the growth and optical characteristics of Ge NCs formed within HfO_2 by Ge^- ion implantation and annealing.

A 5 nm SiO_2 layer was first grown on *p*-type (100) Si wafer by conventional thermal oxidation. A 25 nm HfO_2 layer was then grown on top of the SiO_2 layer by atomic layer deposition. These $Si/SiO_2/HfO_2$ structures were implanted at room temperature (RT) with Ge^- ions of 15 keV to nominal fluences (n_{Ge}) of 8.4×10^{15}, 1.7×10^{16}, and 2.5×10^{16} cm^{-2} and subsequently annealed at temperatures (T_A) in the range from 600 to 1000 °C for 5 min in a N_2 atmosphere. The peak excess Ge concentration for these implants was calculated from TRIM simulation to be around 27 at. % for the highest fluence employed.[10] X-ray photoelectron spectroscopy (XPS) measurements were carried out at RT in the energy of 250 eV at the 7B1 beamline of Pohang Accelerator Laboratory with a base pressure of 1.5×10^{-10} torr. Details of the XPS measurements are described elsewhere.[11] PL (photoluminescence) sectra were measured at 15 K using the 488 nm line of an Ar^+ laser as the excitation source and a liquid nitrogen cooled Ge detector. Standard lock-in detection techniques were used to maximize the signal-to-noise ratio. The laser beam diameter was about 300 μm and the power was about 50 mW.

Figure 1 shows XPS spectra of Ge 3*d* and O 2*s* core levels for Ge-implanted HfO_2 (HfO_2:Ge) with a Ge fluence of 8.4×10^{15} cm^{-2} before and after annealing. The as-implanted sample shows XPS peaks of Ge 3*d* and O 2*s* levels at 30.8 and 23.2 eV, respectively.[12] Five oxidation states, Ge^{n+} ($n=0-4$) responsible for the Ge 3*d* XPS peak could exist in Ge-implanted oxides.[12–14] The Ge 3*d* XPS peaks from crystalline Ge and GeO_2 are usually observed at ~29.3 and ~32.5 eV, respectively, as indicated in Fig. 1.[12] The shift of the Ge 3*d* peak (with respect to Ge^0) has previously been attributed to Ge–O, Ge–Hf–O and Ge–Hf bonds, as

a)Author to whom correspondence should be addressed. Electronic mail: sukho@khu.ac.kr.

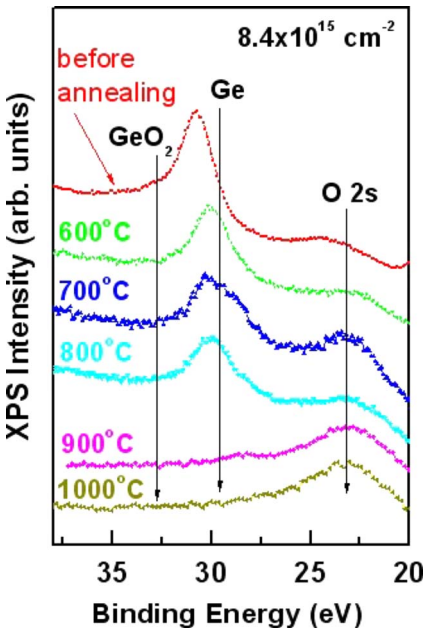

FIG. 1. (Color online) XPS spectra of Ge 3*d* and O 2*s* core levels for HfO_2:Ge films with a Ge fluence of 8.4×10^{15} cm^{-2} before and after annealing.

shown in a study of the Ge/HfO_2 interface[12] or to Ge suboxides.[13,14] The Ge 3*d* XPS peak (30.8 eV) from the as-implanted sample is also therefore attributed to the Ge suboxide phase and/or Ge–Hf–O/Ge–Hf bonds. After annealing at 600 °C the Ge 3*d* peak shifts to lower energy, consistent with the formation of elemental-Ge NCs. Similar peaks are observed for samples annealed at temperatures in the range from 600 to 800 °C suggesting that stable Ge NCs are formed in this temperature range. However, for $T_A \geq 900$ °C the Ge 3*d* peak disappears, suggesting that Ge is no longer present in the near surface region.

Figure 2 compares infrared (IR) PL spectra from Ge-implanted HfO_2 after annealing at 700 °C with those of untreated and annealed HfO_2 layers. The 1.03 eV PL peak observed in unimplanted and implanted HfO_2 samples is attributed to native defects in HfO_2, possibly including metallic Hf,[13] and the 1.10 and 1.13 eV peaks are attributed to the transverse optical (TO_{Si}) and acoustical (TA_{Si}) transitions in the Si substrate, respectively. Two additional peaks are observed for Ge-implanted samples, one at 0.94 and one at 0.88 eV. These are most evident for the sample implanted with 8.4×10^{15} Ge cm^{-2} and are observed to redshift and decrease in intensity as the Ge implant fluence is increased. The two peaks are attributed to the no-phonon (NP_{NC}) and transverse-optical (TO_{NC}) phonon replica from Ge NCs, respectively, as reported for Ge NCs in SiO_2.[15] The observed redshift and the reduction in intensity can be attributed to an increase in the average size of Ge NCs at higher implant fluences.[15] Visible PL emission is also observed from these samples but this is not readily correlated with the presence of the NCs.

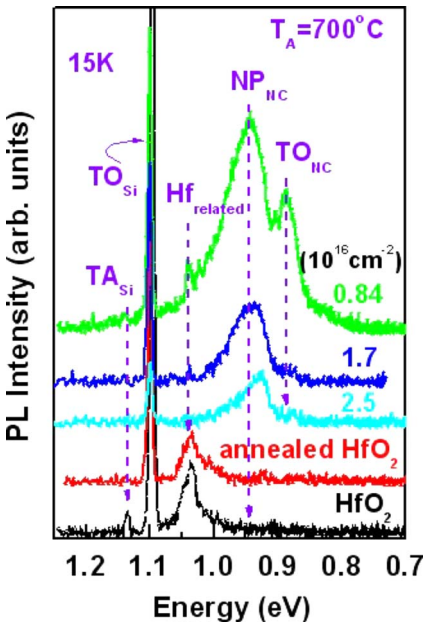

FIG. 2. (Color online) IR PL spectra of HfO_2:Ge films at each n_{Ge} after annealing at 700 °C together with those of untreated and annealed HfO_2 layers.

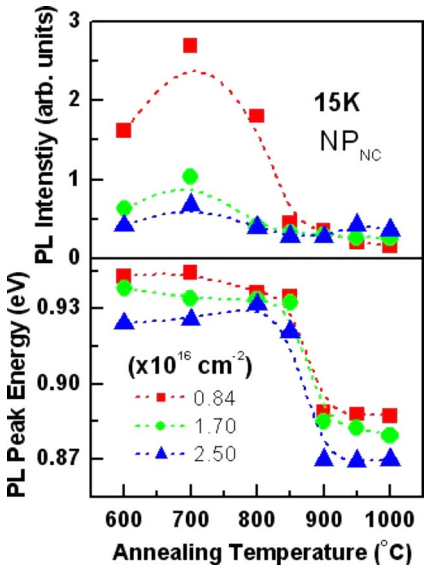

FIG. 3. (Color online) Annealing temperature-dependent PL peak intensities and energies of HfO_2:Ge films at each n_{Ge}.

Figure 3 summarizes the effect of annealing temperature on the Ge-related PL emission (i.e., the NP_{NC} peak). The data clearly show that the PL intensity increases for samples annealed at temperatures up to 700 °C and then decreases rapidly for samples annealed at higher temperatures, and that the emission also undergoes a significant redshift for temperatures above 800 °C. Both of these effects are consistent with an increase in the average size of Ge NCs at higher temperatures.[8] The synthesis of Ge NCs proceeds by nucleation, growth, and Ostwald ripening, and depends on the solubility and diffusivity of Ge in the host material and on the Ge concentration, concentration profile, annealing temperature, and annealing ambient.[7,9] The optimum temperature for the formation of Ge NCs in SiO_2 is known to be within the range of the bulk melting point $(\sim937)\pm235$ °C.[16] The present study shows that this temperature is much lower (i.e., 600–700 °C) in HfO_2.

Figure 4(a) shows cross-sectional high-resolution transmission electron microscopy (HRTEM) images taken along the (110) zone axis of a HfO_2 grain for a sample implanted

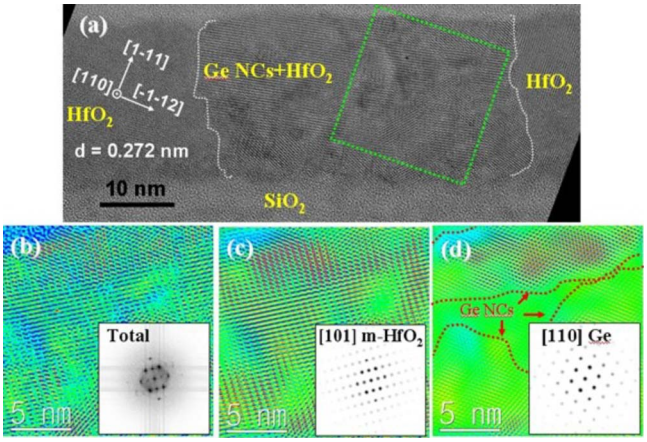

FIG. 4. (Color online) (a) Cross-sectional HRTEM image taken along the (110) zone axis for HfO_2:Ge films with a fluence of 8.4×10^{15} cm^{-2} after annealing at 700 °C. [(b)–(d)] IFFT images and diffractograms (insets) corresponding to *m*-HfO_2+Ge NC, *m*-HfO_2, and Ge NC, respectively.

with 8.4×10^{15} Ge cm^{-2} after annealing at 700 °C. The HfO_2:Ge layer consists of nanocrystalline grains having a lattice spacing *d* of about 0.272 nm and corresponding to the monoclinic (*m*–) phase of typical HfO_2.[5] This particular grain contains Ge NCs, which are more clearly delineated in the processed images depicted in Figs. 4(b)–4(d). Specifically, Fig. 4(b) shows an enlarged image of the region defined by the square together with its diffractogram (as an inset), which represents the superimposition of images from *m*-HfO_2 and Ge NCs. Fourier mask filtering techniques[17] were employed to distinguish the Ge NCs from the *m*-HfO_2 and the filtered diffractograms and HRTEM images from their inverse fast Fourier transforms (IFFTs) reflect the separated image amplitudes generated from the [101] *m*-HfO_2 and [110] Ge NC, as shown in Figs. 4(c) and 4(d), respectively. The IFFT result of [101] *m*-HfO_2 in Fig. 4(c) is similar to that of the composite image in Fig. 4(b), indicating that the matrix can be regarded as *m*-HfO_2 structure. However, the HRTEM image generated from the IFFT of [110] Ge diffractogram shows regions of confined image amplitude within several tens nanometers corresponding to the Ge NC, as indicated by the dotted lines in Fig. 4(d). These results suggest that implanted Ge forms Ge NCs within the matrix of *m*-HfO_2 during thermal annealing with the orientation relationship of [101]*m*-HfO_2//[110]Ge NC.

These nanostructures are repeated through the whole area of the samples, as confirmed by HRTEM. For samples annealed at 700 °C, the average size of the Ge NCs was estimated to be $\sim13.5\pm2.6$ nm for a Ge fluence of 8.4×10^{15} cm^{-2}, and increased monotonically with increasing Ge fluence to $\sim20.0\pm3.7$ nm for a fluence of 2.5×10^{16} cm^{-2}. These NC sizes are much larger than within amorphous SiO_2. Before annealing, the HfO_2:Ge shows two secondary ion mass spectrometry (SIMS) peaks, (the data were not shown here) among which one in HfO_2 layer is much larger than the other in SiO_2 layer. During annealing, the Ge atoms within HfO_2 form Ge NCs while the Ge SIMS peak moves a very slight distance of ~1.5 nm toward the HfO_2/SiO_2 interface with almost no change of its intensity, indicating little long-range diffusion of Ge atoms within HfO_2. In contrast, the Ge SIMS peak within SiO_2 diffuses considerably to the SiO_2/Si interface or even into the Si substrate by the annealing. Ge NCs or NDs usually show nonuniform distribution of size and density within SiO_2 due to the high diffusion rate of Ge atoms,[8,9] consistent with our results. The crystallization of HfO_2 would facilitate the aggregation of Ge atoms by driving them away from the HfO_2 region, resulting in the NC formation at lower temperature as ~700 °C. In addition to this effect, the little long-range diffusion of Ge atoms within HfO_2 would also help Ge NCs grow larger than within SiO_2.

In summary, Ge NCs were formed within HfO_2 by Ge^--ion implantation and relatively low temperature (600–700 °C) annealing. As the implant fluence increased from 8.4×10^{15} to 2.5×10^{16} cm^{-2} the size of the Ge NCs increased from 13.5 ± 2.6 to $\sim20.0\pm3.7$ nm. These NC sizes are much larger than within amorphous SiO_2. PL emission attributable to the Ge NCs was observed in the implanted and annealed samples and this was shown to have a maximum intensity after annealing at 700 °C. The PL emission exhibited a redshift and a reduction in intensity as the average size of the NCs increased for annealing temperatures above 700 °C. Implanted Ge was shown to form Ge NCs within the matrix of *m*-HfO_2 with the orientation relationship of [101]*m*-HfO_2//[110]Ge NC.

S.H.C. and R.G.E. acknowledge supports from the Korea Research Foundation Grant (Grant No. KRF-2007-521-C00094) and from the Australian Research Council (Discovery Project), respectively.

[1] K. I. Han, Y. M. Park, S. Kim, S.-H. Choi, K. J. Kim, I. H. Park, and B.-G. Park, IEEE Trans. Electron Devices **54**, 359 (2007).
[2] C. J. Park, H. Y. Cho, S. Kim, S.-H. Choi, R. G. Elliman, J. H. Han, C. Kim, H. N. Hwang, and C. C. Hwang, Appl. Phys. Lett. **99**, 036101 (2006).
[3] K. S. Seol, K. S. Cho, B.-K. Kim, J.-Y. Choi, E.-K. Lee, Y.-S. Min, J.-B. Park, and S.-H. Choi, J. Korean Phys. Soc. **50**, 49 (2007).
[4] M. Kanoun, A. Souifi, T. Baron, and F. Mazen, Appl. Phys. Lett. **84**, 5079 (2004).
[5] J. E. Jaffe, R. A. Bachorz, and M. Gutowski, Phys. Rev. B **72**, 144107 (2005).
[6] K.-I. Seo, D.-I. Lee, P. Pianetta, H. Kim, K. C. Saraswat, and P. C. McIntyre, Appl. Phys. Lett. **89**, 142912 (2006).
[7] F. Zheng, H. G. Chew, W. K. Choi, J. X. Zhang, and H. L. Seng, J. Appl. Phys. **101**, 114310 (2007).
[8] X. L. Wu, T. Gao, X. M. Bao, F. Yan, S. S. Jiang, and D. Feng, J. Appl. Phys. **82**, 2704 (1997).
[9] W. K. Choi, V. Ho, V. Ng, Y. W. Ho, S. P. Ng, and W. K. Chim, Appl. Phys. Lett. **86**, 143114 (2005).
[10] J. P. Biersack and L. G. Haggmark, Nucl. Instrum. Methods **174**, 257 (1980).
[11] S. Kim, M. C. Kim, S.-H. Choi, K. J. Kim, H. N. Hwang, and C. C. Hwang, Appl. Phys. Lett. **91**, 103113 (2007).
[12] J. Zuk, H. Krzyzanowska, M. J. Clouter, M. Bromberek, H. Bubert, L. Rebohle, and W. Skorupa, J. Appl. Phys. **96**, 4952 (2004).
[13] G. Pourtois, M. Houssa, A. Delable, T. Conard, M. Caymax, M. Meuris, and M. M. Heyns, Appl. Phys. Lett. **92**, 032105 (2008).
[14] A. Molle, Md. N. K. Bhulyan, G. Tallarida, and M. Fanclulli, Appl. Phys. Lett. **89**, 083504 (2006).
[15] S. Takeoka, M. Fujji, S. Hayashi, and K. Yamamoto, Phys. Rev. B **58**, 7921 (1998).
[16] Q. Xu, L. D. Sharp, C. W. Yuan, D. O. Yi, C. Y. Liao, A. M. Glaeser, A. M. Minor, J. W. Beeman, M. C. Ridgway, P. Kluth, J. W. Ager III, D. C. Chrzan, and E. E. Haller, Phys. Rev. Lett. **97**, 155701 (2006).
[17] Y.-M. Kim, J.-M. Jeong, J.-G. Kim, Y.-J. Kim, and Y. S. Lim, J. Korean Phys. Soc. **48**, 250 (2006).